

Hydride Transfer from 9-Substituted 10-Methyl-9,10-dihydroacridines to Hydride Acceptors via Charge-Transfer Complexes and Sequential Electron–Proton–Electron Transfer. A Negative Temperature Dependence of the Rates

Shunichi Fukuzumi,* Kei Ohkubo, Yoshihiro Tokuda, and Tomoyoshi Suenobu

Contribution from the Department of Material and Life Science, Graduate School of Engineering, Osaka University, CREST, Japan Science and Technology Corporation, Suita, Osaka 565-0871, Japan

Received November 29, 1999

Abstract: The reactivity of 9-substituted 10-methyl-9,10-dihydroacridine (AcrHR) in the reactions with hydride acceptors (A) such as *p*-benzoquinone derivatives and tetracyanoethylene (TCNE) in acetonitrile varies significantly spanning a range of 10^7 starting from R = H to Bu' and CMe₂COOMe. Comparison of the large variation in the reactivity of the hydride transfer reaction with that of the deprotonation of the radical cation (AcrHR^{•+}) determined independently indicates that the large variation in the reactivity is attributed mainly to that of proton transfer from AcrHR^{•+} to A^{•-} following the initial electron transfer from AcrHR to A. The overall hydride transfer reaction from AcrHR to A therefore proceeds via sequential electron–proton–electron transfer in which the initial electron transfer to give the radical ion pair (AcrHR^{•+} A^{•-}) is in equilibrium and the proton transfer from AcrHR^{•+} to A^{•-} is the rate-determining step. Charge-transfer complexes are shown to be formed in the course of the hydride transfer reactions from AcrHR to *p*-benzoquinone derivatives. A negative temperature dependence was observed for the rates of hydride transfer reactions from AcrHR (R = H, Me, and CH₂Ph) to 2,3-dichloro-5,6-dicyano-*p*-benzoquinone (DDQ) in chloroform (*the lower the temperature, the faster the rate*) to afford the negative activation enthalpy ($\Delta H_{\text{obs}}^{\ddagger} = -32, -4, \text{ and } -13 \text{ kJ mol}^{-1}$, respectively). Such a negative $\Delta H_{\text{obs}}^{\ddagger}$ value indicates clearly that the CT complex lies along the reaction pathway of the hydride transfer reaction via sequential electron–proton–electron transfer and does not enter merely through a side reaction that is indifferent to the hydride transfer reaction. The $\Delta H_{\text{obs}}^{\ddagger}$ value increases with increasing solvent polarity from a negative value (-13 kJ mol^{-1}) in chloroform to a positive value (13 kJ mol^{-1}) in benzonitrile as the proton-transfer rate from AcrHR^{•+} to DDQ^{•-} may be slower.

Introduction

Dihyronicotinamide adenine dinucleotide (NADH) and analogues act as the source of two electrons and a proton, thus formally transferring a hydride ion to a suitable substrate.¹ The mechanism of the hydride transfer has so far been extensively studied by using NADH analogues in the reactions with various substrates.^{2–12} In these investigations, the mechanism has been

discussed concerning two main possibilities, i.e., concerted hydride transfer or sequential electron–proton–electron (equivalent to a hydride ion) transfer. Since both processes involve the formation of a formal positive charge in the transition state, it has been difficult to differentiate between the mechanisms based on the classical approach of electronic and substitution effects.^{13–15} We have previously reported that the distinction between the

(1) Stryer, L. *Biochemistry*, 3rd ed; Freeman: New York, 1988; Chapter 17.

(2) (a) Eisner, U.; Kuthan, J. *Chem. Rev.* **1972**, *72*, 1. (b) Stout, D. M.; Meyer, A. I. *Chem. Rev.* **1982**, *82*, 223.

(3) Fukuzumi, S.; Tanaka, T. *Photoinduced Electron Transfer*; Fox, M. A., Chanon, M., Eds.; Elsevier: Amsterdam, 1988; Part C, Chapter 10.

(4) (a) Sund, H. *Pyridine-Nucleotide Dependent Dehydrogenase*; Walter de Gruyter: West Berlin, 1977. (b) Kellog, R. M. *Top. Curr. Chem.* **1982**, *101*, 111. (c) Kellog, R. M. *Angew. Chem.* **1984**, *96*, 769. (d) Ohno, A.; Ushida, S. *Lecture Notes in Bioorganic Chemistry. Mechanistic Models of Asymmetric Reductions*; Springer-Verlag: Berlin, 1986; p 105. (e) Bunting, J. W. *Bioorg. Chem.* **1991**, *19*, 456. (f) He, G.-X.; Blasko, A.; Bruice, T. C. *Bioorg. Chem.* **1993**, *21*, 423. (g) Ohno, A. *J. Phys. Org. Chem.* **1995**, *8*, 567.

(5) Fukuzumi, S. *Advances in Electron-Transfer Chemistry*; Mariano, P. S., Ed.; JAI Press: Greenwich, CT, 1992; pp 67–175.

(6) Fukuzumi, S.; Koumitsu, S.; Hironaka, K.; Tanaka, T. *J. Am. Chem. Soc.* **1987**, *109*, 305 and references therein.

(7) (a) Fukuzumi, S.; Ishikawa, M.; Tanaka, T. *J. Chem. Soc., Perkin Trans. 2* **1989**, 1811. (b) Fukuzumi, S.; Mochizuki, S.; Tanaka, T. *J. Am. Chem. Soc.* **1989**, *111*, 1497. (c) Ishikawa, M.; Fukuzumi, S. *J. Chem. Soc., Chem. Commun.* **1990**, 1353.

(8) Cheng, J.-P.; Lu, Y.; Zhu, X.; Mu, L. *J. Org. Chem.* **1998**, *63*, 6108.

(9) Ohno, A.; Ishikawa, Y.; Yamazaki, N.; Okamura, M.; Kawai, Y. *J. Am. Chem. Soc.* **1998**, *120*, 1186.

(10) (a) Pestovsky, O.; Bakac, A.; Espenson, J. H. *J. Am. Chem. Soc.* **1998**, *120*, 13422. (b) Pestovsky, O.; Bakac, A.; Espenson, J. H. *Inorg. Chem.* **1998**, *37*, 1616.

(11) Anne, A.; Moiroux, J.; Savéant, J.-M. *J. Am. Chem. Soc.* **1993**, *115*, 10224.

(12) (a) Kreevoy, M. M.; Ostovic, D.; Lee, I.-S. H.; Binder, D. A.; King, G. W. *J. Am. Chem. Soc.* **1988**, *110*, 524. (b) Lee, I.-S. H.; Jeoung, E. H.; Kreevoy, M. M. *J. Am. Chem. Soc.* **1997**, *119*, 2722.

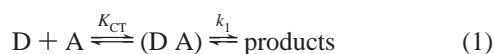
(13) (a) Ohno, A.; Yamamoto, H.; Oka, S. *J. Am. Chem. Soc.* **1981**, *103*, 2041. (b) Ohno, A.; Shio, T.; Yamamoto, H.; Oka, S. *J. Am. Chem. Soc.* **1981**, *103*, 2045.

(14) (a) Powell, M. F.; Bruice, T. C. *J. Am. Chem. Soc.* **1983**, *105*, 1014, 7139. (b) Chipman, D. M.; Yaniv, R.; van Eikeren, P. *J. Am. Chem. Soc.* **1980**, *102*, 3244.

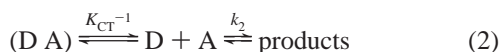
(15) (a) Carlson, B. W.; Miller, L. L. *J. Am. Chem. Soc.* **1985**, *107*, 479. (b) Miller, L. L.; Valentine, J. R. *J. Am. Chem. Soc.* **1988**, *110*, 3982. (c) Colter, A. K.; Plank, P.; Bergsma, J. P.; Lahti, R.; Quesnel, A. A.; Parsons, A. G. *Can. J. Chem.* **1984**, *62*, 1780. (d) Verhoeven, J. W.; van Gerresheim, W.; Martens, F. M.; van der Kerk, S. M. *Tetrahedron* **1986**, *42*, 975. (e) Coleman, C. A.; Rose, J. G.; Murray, C. J. *J. Am. Chem. Soc.* **1992**, *114*, 9755.

two mechanisms can be made by comparing the reactivities of different types of NADH analogues which have different donor abilities in the initial and second electron transfer in the electron-proton-electron sequence.⁶ Namely, the one-electron donor ability between 1-benzyl-1,4-dihydronicotinamide (BNAH) and 10-methyl-9,10-dihydroacridine (AcrH₂) is rather similar, as compared to the large difference in the one-electron donor ability between the corresponding radicals, i.e., BNA• and AcrH•.⁶ In such a case, the energetics of the initial electron transfer is similar, while the energetics of overall hydride transfer is quite different between the two NADH analogues. We have shown clearly that the activation barrier is mainly determined by the energetics of initial electron transfer rather than the energetics of overall hydride transfer.⁶

The mechanistic discussion is further complicated by formation of charge-transfer (CT) complexes in the course of hydride-transfer reactions from NADH analogues to *p*-benzoquinone derivatives and tetracyanoethylene (TCNE).^{16,17} The CT complexes have been implicated as intermediates in a variety of reactions between electron donors (D) and acceptors (A), eq 1.^{18–20} However, the mechanistic involvement of CT complexes



has always been questioned by an alternative mechanism in which the CT complex is merely an innocent bystander in an otherwise dead-end equilibrium, eq 2.²¹ The two pathways in eqs 1 and 2 are kinetically indistinguishable.²² However, Kiselev



and Miller²³ have shown that the two pathways in eqs 1 and 2 can be distinguishable by the temperature dependence of the observed second-order rate constant (k_{obs}) if one can observe a negative temperature dependence. A negative activation enthalpy could only arise when the CT complex lies along the reaction pathway (eq 1), since for such a pathway, $k_{\text{obs}} = k_1 K_{CT} [\Delta H_{\text{obs}}^{\ddagger} = \Delta H_1^{\ddagger} (>0) + \Delta H_{CT} (<0)]$, whereas for the other pathway (eq 2), $k_{\text{obs}} = k [\Delta H_{\text{obs}}^{\ddagger} = \Delta H_2^{\ddagger} (>0)]$. Thus, the necessary condition to observe a negative activation enthalpy for reactions involving CT complexes is that the heat of formation of the CT complex ($\Delta H_{CT} < 0$) is of greater magnitude than the activation enthalpy for the passage of the CT complex to the transition state (ΔH_1^{\ddagger})

(16) Fukuzumi, S.; Nishizawa, N.; Tanaka, T. *J. Org. Chem.* **1984**, *49*, 3571.

(17) Fukuzumi, S.; Kondo, Y.; Tanaka, T. *J. Chem. Soc., Perkin Trans. 2* **1984**, 673.

(18) (a) Mulliken, R. S.; Person, W. B. *Molecular Complexes*; A Lecture and Reprint Volume; Wiley-Interscience: New York, 1969. (b) Foster, R. *Organic Charge-Transfer Complexes*; Academic Press: New York, 1969.

(19) (a) Kochi, J. K. *Adv. Phys. Org. Chem.* **1994**, *29*, 185. (b) Kochi, J. K. *Chimica* **1991**, *45*, 277. (c) Kochi, J. K. *Angew. Chem., Int. Ed. Engl.* **1988**, *27*, 1227. (d) Kochi, J. K. *Acc. Chem. Res.* **1992**, *25*, 39. (d) Kochi, J. K. *Acta Chem. Scand.* **1990**, *44*, 409.

(20) (a) Chanon, M.; Tobe, M. *Angew. Chem., Int. Ed. Engl.* **1982**, *21*, 1. (b) Jones, G., II In *Photoinduced Electron Transfer*; Fox, M. A., Chanon, M., Eds.; Elsevier: Amsterdam, 1988; Part A, p 245. (c) Chanon, M.; Rajzmann, M.; Chanon, F. *Tetrahedron* **1990**, *46*, 6193. (d) Julliard, M.; Chanon, M. *Chem. Rev.* **1983**, *83*, 425.

(21) Sustmann, R.; Korth, H.-G.; Nüchter, U.; Siangouri-Feulner, I.; Sicking, W. *Chem. Ber.* **1991**, *124*, 2811.

(22) (a) Fukuzumi, S.; Mochida, K.; Kochi, J. K. *J. Am. Chem. Soc.* **1979**, *101*, 5961. (b) Fukuzumi, S.; Kochi, J. K. *J. Am. Chem. Soc.* **1980**, *102*, 2141. (c) Fukuzumi, S.; Kochi, J. K. *Tetrahedron* **1982**, *38*, 1035.

(23) Kiselev, V. D.; Miller, J. G. *J. Am. Chem. Soc.* **1975**, *97*, 4036.

(24) A negative temperature dependence of the rates of photoinduced electron-transfer reactions of ruthenium(II) complexes has been reported: (a) Kim, H.-B.; Kitamura, N.; Kawanishi, Y.; Tazuke, S. *J. Am. Chem. Soc.* **1987**, *109*, 2506. (b) Kim, H.-B.; Kitamura, N.; Kawanishi, Y.; Tazuke, S. *J. Phys. Chem.* **1989**, *93*, 5757.

> 0) in eq 1, i.e., $-\Delta H_{CT} > \Delta H_1^{\ddagger}$. However, it is difficult to examine the kinetics in such a system, since formation of strong CT complexes, which is prerequisite to observe negative $\Delta H_{\text{obs}}^{\ddagger}$ values, is usually too fast to follow the reactions. Fine-tuning of the strength of the CT complex and the reactivity seems essential to observe the negative $\Delta H_{\text{obs}}^{\ddagger}$ values.^{24,25}

We have previously shown that 9-substituted 10-methyl-9,10-dihydroacridines (AcrHR) have similar one-electron donor properties but quite different proton donor abilities in the corresponding radical cations formed by the electron-transfer oxidation of AcrHR with Fe³⁺ and that the deprotonation rate varies significantly depending on the substituent R.^{26,27}

In this study we have examined the change in the reactivities of AcrHR having a variety of substituents R in the reactions with hydride acceptors. The present study provides an excellent opportunity to compare the reactivities of AcrHR in the hydride-transfer reactions with those in the deprotonation of the corresponding radical cations. By the proper choice of alkyl (or phenyl) substituents in AcrHR the electron donor property of AcrHR and the acid property of AcrHR⁺ can be systematically varied and finely tuned to cover a wide range of subtle molecular effects. Such fine-tuning of the electron donor and acid properties has enabled us to observe negative activation enthalpies for the hydride-transfer reactions of AcrHR, which indicates unequivocally that the CT complex is a true intermediate for the hydride-transfer reaction, lying on the reaction pathway.²⁸

Experimental Section

Materials. 9,10-Dihydro-10-methylacridine (AcrH₂) was prepared from 10-methylacridinium iodide (AcrH⁺I⁻) by reduction with NaBH₄ in methanol and purified by recrystallization from ethanol.²⁹ AcrH⁺I⁻ was prepared by the reaction of acridine with methyl iodide in acetone and was converted to the perchlorate salt (AcrH⁺ClO₄⁻) by the addition of magnesium perchlorate to the iodide salt (AcrH⁺I⁻) and purified by recrystallization from methanol.⁶ 9-Alkyl (or phenyl)-9,10-dihydro-10-methylacridine (AcrHR; R = Me, Et, CH₂Ph, and Ph) was prepared by the reduction of AcrH⁺I⁻ with the corresponding Grignard reagents (RMgX).²⁷ AcrHR (R = Prⁱ, Bu^t, CHPh₂, and 1-CH₂C₁₀H₇) was prepared by the photoreduction of AcrH⁺ClO₄⁻ with RCOOH in the presence of NaOH in H₂O-MeCN as described previously.³⁰ AcrHR (R = CH₂-COOEt, CMe(H)COOEt, and CMe₂COOMe) was prepared by the reduction of AcrH⁺ClO₄⁻ with the corresponding ketene silyl acetals (CH₂=C(OEt)OSiEt₃, CMe(H)=C(OEt)OSiEt₃, and Me₂C=C(OMe)-OSiMe₃, respectively).³¹ 9-Substituted 10-methylacridinium perchlorate (AcrR⁺ClO₄⁻; R = Me, Et, Prⁱ, Bu^t, CHPh₂, and Ph) was prepared by the reaction of 10-methylacridone in dichloromethane with the corresponding Grignard reagents (RMgX) and purified by recrystallization from ethanol-diethyl ether.³² *p*-Benzoquinone derivatives (2,3-dichloro-5,6-dicyano-*p*-benzoquinone (DDQ), *p*-chloranil, 2,6-dichloro-*p*-benzoquinone, and chloro-*p*-benzoquinone) and tetracyanoethylene (TCNE)

(25) Brominations of some alkenes in nonpolar media were reported to have negative activation energies: Sergeev, G. B.; Serguchev, Yu. A.; Smirnov, V. V. *Russ. Chem. Rev.* **1973**, *42*, 697.

(26) (a) Fukuzumi, S.; Kitano, T. *Chem. Lett.* **1990**, 1275. (b) Fukuzumi, S.; Mochizuki, S.; Tanaka, T. *J. Chem. Soc., Dalton Trans.* **1990**, 695.

(27) Fukuzumi, S.; Tokuda, Y.; Kitano, T.; Okamoto, T.; Otera, J. *J. Am. Chem. Soc.* **1993**, *115*, 8960.

(28) A preliminary report on the observation of a negative activation enthalpy for a hydride transfer reaction of a hydride donor other than NADH analogues has appeared: (a) Zaman, K. M.; Yamamoto, S.; Nishimura, N.; Maruta, J.; Fukuzumi, S. *J. Am. Chem. Soc.* **1994**, *116*, 12099. (b) Yamamoto, S.; Sakurai, T.; Liu, Y.; Sueishi, Y. *Phys. Chem. Chem. Phys.* **1999**, *1*, 833.

(29) Roberts, R. M. G.; Ostovic, D.; Kreevoy, M. M. *Faraday Discuss. Chem. Soc.* **1982**, *74*, 257.

(30) Fukuzumi, S.; Kitano, T.; Tanaka, T. *Chem. Lett.* **1989**, 1231.

(31) Otera, J.; Wakahara, Y.; Kamei, H.; Sato, T.; Nozaki, H.; Fukuzumi, S. *Tetrahedron Lett.* **1991**, *32*, 2405.

(32) Bernthsen, A. *Ann.* **1884**, *224*, 1.

were obtained commercially and purified by the standard methods.³³ Acetonitrile and benzonitrile used as a solvent were purified and dried by the standard procedure.³³ Chloroform and 1,2-dichloroethane (spectral grade) were obtained commercially from Wako Pure Chemicals and used without further purification.

Reaction Procedure. Typically, AcrHR (4.0×10^{-2} M) and DDQ (6.0×10^{-2} M) were added to an NMR tube that contained deaerated CD₃CN solution (0.60 cm³) under an atmospheric pressure of argon. The oxidized products of AcrHR were identified by the ¹H NMR spectra by comparing with those of authentic samples. The ¹H NMR measurements were performed using a JNM-GSX-400 (400 MHz) NMR spectrometer. ¹H NMR (CD₃CN): AcrMe⁺ClO₄⁻, δ 3.48 (s, 3H), 4.74 (s, 3H), 7.9–8.9 (m, 8H); AcrEt⁺ClO₄⁻, δ 1.52 (t, 3H, *J* = 7.5 Hz), 3.95 (q, 2H), 4.71 (s, 3H), 7.9–8.9 (m, 8H); AcrPh⁺ClO₄⁻, δ 4.83 (s, 3H), 7.5–8.6 (m, 13H); AcrCH₂Ph⁺ClO₄⁻, δ 4.79 (s, 3H), 5.35 (s, 2H), 7.5–8.9 (m, 13H); AcrCHPh₂⁺ClO₄⁻, δ 4.70 (s, 3H), 5.96 (s, 1H), 7.5–8.9 (m, 18H); Acr(1-CH₂C₁₀H₇)⁺ClO₄⁻, δ 4.80 (s, 3H), 5.72 (s, 2H), 7.5–8.9 (m, 15H); AcrCH₂COOEt⁺ClO₄⁻, δ 1.09 (t, 3H, *J* = 8.0 Hz), 2.41 (q, 2H, *J* = 8.0 Hz), 4.76 (s, 3H), 5.02 (s, 2H), 7.7–8.7 (m, 8H).

Spectral and Kinetic Measurements. The reactions of AcrHR with DDQ and TCNE in deaerated MeCN were monitored with a Shimadzu UV-2200, 160A spectrophotometer or a Hewlett-Packard 8453 diode array spectrophotometer when the rates were slow enough to be determined accurately. The rates were determined from appearance of the absorbance due to AcrR⁺ ($\lambda_{\max} = 358$ nm, $\epsilon_{\max} = 1.80 \times 10^4$ M⁻¹ cm⁻¹) or the radical anion (DDQ^{•-}: $\lambda_{\max} = 585$ nm, $\epsilon_{\max} = 5.6 \times 10^3$ M⁻¹ cm⁻¹; TCNE^{•-}: $\lambda_{\max} = 457$ nm, $\epsilon_{\max} = 5.67 \times 10^3$ M⁻¹ cm⁻¹).^{34,35} The kinetic measurements for faster reactions such as the reaction of AcrH₂ or AcrHCH₂Ph with DDQ were carried out with a Union RA-103 stopped-flow spectrophotometer which was thermostated at 298 K under deaerated conditions. The concentration of AcrHR or a hydride acceptor was maintained at more than 15-fold excess of the other reactant to attain pseudo-first-order conditions. Pseudo-first-order rate constants were determined by a least-squares curve fit using an NEC microcomputer. The first-order plots of $\ln(A_{\infty} - A)$ vs time (A_{∞} and *A* are the final absorbance and the absorbance at the reaction time, respectively) were linear for three or more half-lives with the correlation coefficient $\rho > 0.999$. In each case, it was confirmed that the rate constants derived from at least five independent measurements agreed within an experimental error of $\pm 5\%$.

The transient CT spectra of complexes formed between AcrHR and *p*-benzoquinone derivatives with half-lives <10 s were obtained by plotting the initial rise of the absorbance against the wavelength with a stopped flow spectrophotometer. The CT spectra of stable complexes such as the AcrHCH₂Ph–chloro-*p*-benzoquinone complex were measured with a Hewlett-Packard 8452 or a Hewlett-Packard 8453 diode array spectrophotometer. The formation constant (K_{CT}) of the AcrHCH₂Ph–chloro-*p*-benzoquinone complex was determined from the dependence of the initial rise of the absorbance at $\lambda_{\max} = 530$ nm due to the CT complex on the concentration of chloro-*p*-benzoquinone in MeCN at various temperatures.

The ESR spectra of DDQ^{•-} and TCNE^{•-} formed as final products in the reactions of AcrHR with DDQ and TCNE, respectively, were measured with a JEOL X-band spectrometer (JES-RE1XE). The *g* values and the hyperfine coupling constants were calibrated with a Mn²⁺ marker.

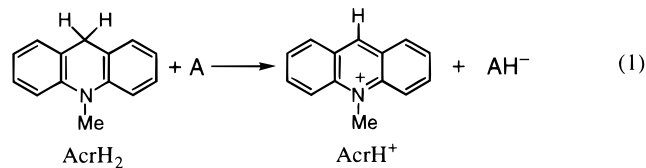
Cyclic Voltammetry. Cyclic voltammetry measurements were performed at 298 K on a BAS 100 W electrochemical analyzer in deaerated MeCN containing 0.1 M Bu₄NClO₄ (TBAP) as supporting electrolyte. A conventional three-electrode cell was used with a platinum working electrode (surface area of 0.3 mm²) and a platinum wire as the counter electrode. The Pt working electrode (BAS) was routinely polished with a BAS polishing alumina suspension and rinsed with acetone before use. The measured potentials were recorded with respect to the Ag/AgNO₃ (0.01 M) reference electrode. All potentials (vs Ag/

Ag⁺) were converted to values vs SCE by adding 0.29 V.³⁶ All electrochemical measurements were carried out under an atmospheric pressure of argon.

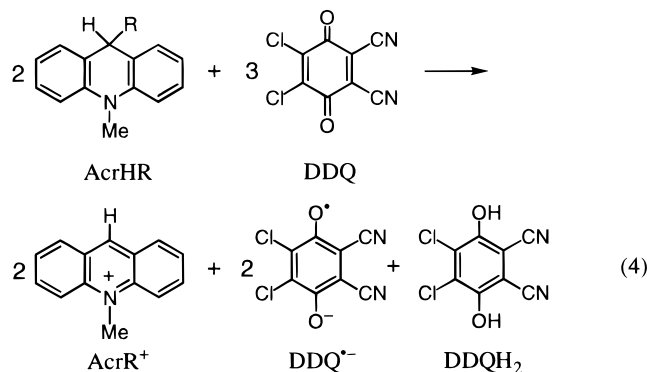
Theoretical Calculations. Theoretical calculations were performed using the MOPAC program (Ver. 6) which is incorporated in the MOLMOLIS program (Ver. 2.8) by Daikin Industries, Co. Ltd. The PM3 Hamiltonian was used for the semiempirical MO calculations.³⁷ Final geometries and energetics were obtained by optimizing the total molecular energy with respect to all structural variables. The heats of formation (ΔH_f) were calculated with the restricted Hartree–Fock (RHF) formalism using a key word “PRECISE”.

Results and Discussion

Reactions of AcrHR with Hydride Acceptors. It has previously been reported that hydride transfer reactions from 10-methyl-9,10-dihydroacridine (AcrH₂) as well as 1-benzyl-1,4-dihydronicotinamide (BNAH) to hydride acceptors (A) such as *p*-benzoquinone derivatives^{6,38} and tetracyanoethylene (TCNE)^{17,38} occur efficiently (eq 1) followed by a subsequent fast electron transfer from the reduced product (AH⁻) to A (eq 2) and the disproportionation of the resulting radical (eq 3).



When AcrH₂ is replaced by 9-substituted analogues (AcrHR), essentially the same reactions (eqs 1–3) occur to give the overall stoichiometry as given by eq 4. A typical example of the UV–



vis spectral change in the reaction of AcrHCH₂Ph with DDQ is shown in Figure 1. The spectral titration shown in Figure 2 where $[\text{DDQ}^{\bullet-}]/[\text{DDQ}]_0$ is plotted against $[\text{AcrHR}]/[\text{DDQ}]_0$ confirms the stoichiometry in eq 4 where 2 equiv of AcrHR reacts with 3 equiv of DDQ to yield 2 equiv of DDQ^{•-} (67% yield). The formation of DDQ^{•-} was also confirmed by the ESR spectrum (*g* = 2.0054), which showed the hyperfine structure

(33) Perrin, D. D.; Armarego, W. L. F. *Purification of Laboratory Chemicals*; Butterworth-Heinemann: Oxford, 1988.

(34) Iida, Y. *Bull. Chem. Soc. Jpn.* **1971**, *44*, 1777.

(35) Webster, O. W.; Mahler, W.; Benson, R. E. *J. Am. Chem. Soc.* **1962**, *84*, 3678.

(36) Mann, C. K.; Barnes, K. K. *Electrochemical Reactions in Non-aqueous Systems*; Marcel Dekker: New York, 1990.

(37) Stewart, J. J. P. *J. Comput. Chem.* **1989**, *10*, 209, 221.

(38) (a) Colter, A. K.; Saito, G.; Sharom, F. J.; Hong, A. P. *J. Am. Chem. Soc.* **1976**, *98*, 7833. (b) Colter, A. K.; Saito, G.; Sharom, F. J. *Can. J. Chem.* **1977**, *55*, 2741.

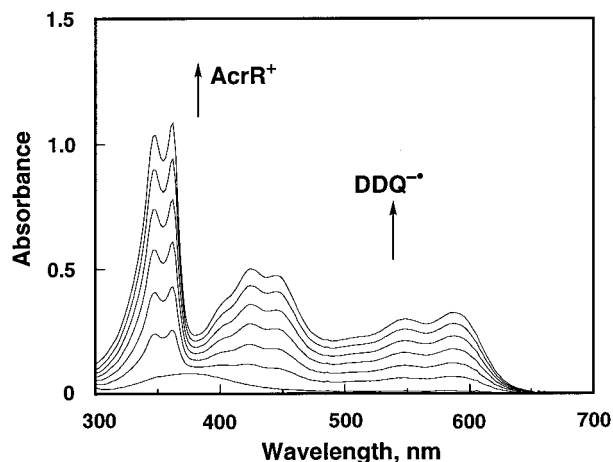


Figure 1. Electronic absorption spectra observed in the reaction of AcrHCH₂Ph ($0, 9.3 \times 10^{-6}, 2.8 \times 10^{-5}, 3.7 \times 10^{-5}, 4.7 \times 10^{-5}, 5.6 \times 10^{-5}, 6.5 \times 10^{-5},$ and 7.5×10^{-5} M) with DDQ (8.3×10^{-5} M) in deaerated MeCN at 298 K.

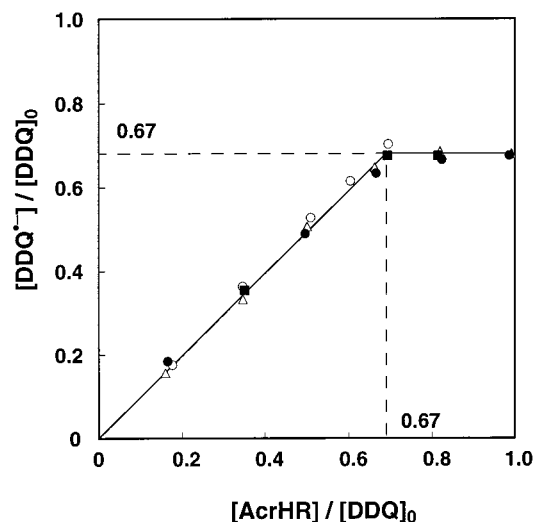


Figure 2. Plot of the ratio of the DDQ⁻ concentration to the initial concentration of DDQ (1.0×10^{-4} M), $[\text{DDQ}^-]/[\text{DDQ}]_0$ vs the ratio of the initial concentration of AcrHR to DDQ, and $[\text{AcrHR}]/[\text{DDQ}]_0$ for the reaction of AcrHR (R = Me (○), CH₂COOEt (●), 1-CH₂C₁₀H₇ (△), and CMe(H)COOEt (■)) with DDQ.

due to two equivalent nitrogens ($a_N = 0.058$ mT) in agreement with the literature value.³⁹ The same 2:3 stoichiometry was obtained for the reaction of AcrHR with TCNE to yield TCNE⁻, the formation of which was confirmed by the absorption spectrum as well as the ESR spectrum.^{17,35,40}

The rates of formation of the radical anion (A⁻) in the presence of a large excess of AcrHR or the hydride acceptor (A) obeyed the pseudo-first-order kinetics.⁴¹ The value of the pseudo-first-order rate constant ($k^{(1)}$) in an excess of AcrHR (eq 5) is 1.5-fold larger than the $k^{(1)}$ value in an excess of A at the same concentration (eq 6). A typical example is shown in Figure 3, where the $k^{(1)}$ values are plotted against [AcrHMe] or [DDQ]. This agrees with the stoichiometry in eq 4 used in excess for the reaction of AcrHMe with DDQ. Thus, the slope of the

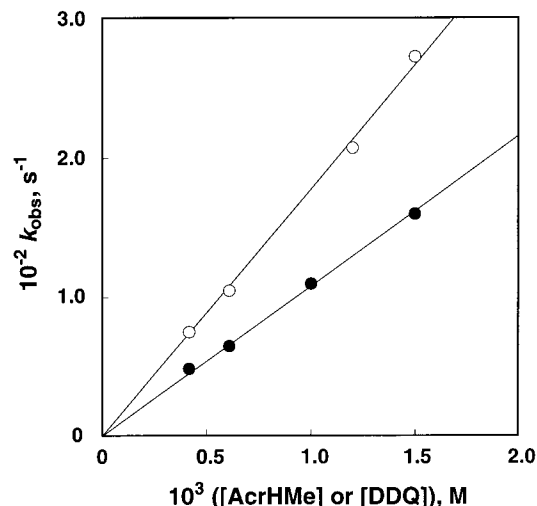


Figure 3. Plots of the pseudo-first-order rate constants ($k^{(1)}$) vs [AcrHMe] (○) or [DDQ] (●) for formation of DDQ⁻ in the reaction of AcrHMe with DDQ in MeCN at 298 K. Either AcrHMe or DDQ is used in a large excess.

Table 1. Rate Constants (k_d) for Deprotonation of AcrHR⁺, One-Electron Oxidation Potentials (E_{ox}^0) of AcrHR, and Rate Constants (k_{obs}) of Hydride Transfer Reactions from AcrHR to DDQ and TCNE in MeCN at 298 K

AcrHR, R =	k_d , s ⁻¹	E_{ox}^0 (vs SCE), ^a V	k_{obs} , M ⁻¹ s ⁻¹	
			DDQ	TCNE
H	6.4	0.81	1.5×10^6	1.0×10^2
Me	1.1	0.84	1.1×10^5	7.0
Ph	4.1	0.88	6.5×10^4	7.9×10^{-1}
Et	0.49	0.84	4.0×10^4	3.0
CH ₂ Ph	0.17 ^b	0.84	1.1×10^4	5.4×10^{-1}
CH ₂ C ₁₀ H ₇	<i>c</i>	0.85	6.9×10^3	3.3×10^{-1}
CH ₂ COOEt	<i>c</i>	0.89	6.9×10^3	2.3×10^{-1}
CHPh ₂	<i>c</i>	0.84	5.3×10^2	1.5×10^{-2}
Pr ⁱ	<i>c</i>	0.84	4.5×10	7.0×10^{-4}
CMe(H)COOEt	<i>c</i>	0.92	2.0×10	3.4×10^{-3}
Bu ⁱ	<i>c</i>	0.86	1.3×10^{-1}	$<5 \times 10^{-5}$
CMe ₂ COOMe	<i>c</i>	0.92	1.3×10^{-1}	$<1 \times 10^{-4}$

^a Taken from ref 27. ^b The deprotonation rate constant separated from the rate constant for the C–C bond cleavage of AcrHCH₂Ph⁺; see ref 43. ^c Too small to be separated from the rate constant for the C–C bond cleavage of AcrHR⁺ accurately.

plot of $k^{(1)}$ vs [A] gives the rate constant (k_{obs}) of the hydride transfer from AcrHR to A (eq 5), and the slope of $k^{(1)}$ vs [AcrHR] gives $(3/2)k_{\text{obs}}$ (eq 6).

$$k^{(1)} = k_{\text{obs}}[\text{A}] \quad (5)$$

$$k^{(1)} = (3/2)k_{\text{obs}}[\text{AcrHR}] \quad (6)$$

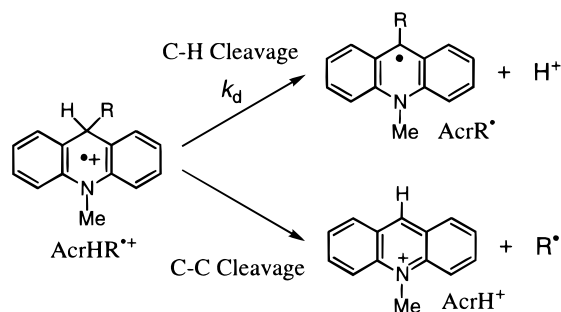
The k_{obs} values for the reactions of a series of AcrHR with hydride acceptors (DDQ and TCNE) are listed in Table 1. The k_{obs} values for the reactions of AcrHR with DDQ vary significantly depending on the substituent R in AcrHR. The magnitude spans a range of 10^7 starting from R = H to Buⁱ and CMe₂COOMe. Similar change in the reactivity with R is observed for the reactions of AcrHR with TCNE (Table 1). Such a significant decrease in the reactivity by the introduction of a substituent at the C-9 position can hardly be reconciled by a concerted hydride transfer mechanism. The alkyl or phenyl group at the C-9 position is known to be in a boat axial conformation, and thereby the hydrogen at the C-9 position is located at the equatorial position, where steric hindrance due

(39) (a) Gordon, D.; Hove, M. J. *J. Chem. Phys.* **1973**, *59*, 3419. (b) Corvaja, C.; Pasimeni, L.; Brustalon, M. *Chem. Phys.* **1976**, *14*, 177. (c) Grampp, G.; Landgraf, S.; Rasmussen, K. *J. Chem. Soc., Perkin Trans. 2* **1999**, 1897.

(40) Phillips, W. D.; Powell, J. C.; Weissman, S. I. *J. Chem. Phys.* **1960**, *33*, 626.

(41) It was confirmed that the rates were not affected by the room light.

Scheme 1



to the axial substituent is minimized in the hydride transfer reactions. Moreover, the introduction of an electron-donating substituent such as $R = \text{Bu}^t$ would activate the release of a negatively charged hydride ion if the concerted hydride transfer should take place. The remarkable decrease in the reactivity with the increasing electron-donor ability of R (Table 1) rather indicates that the reactivity is determined by the process in which a positive charge is released.

Comparison of the Reactivities in Hydride Transfer Reactions of AcrHR and Deprotonation of AcrHR²⁺. We have previously succeeded in detecting transient absorption and ESR spectra of AcrHR²⁺ produced by the electron-transfer oxidation of AcrHR with [Fe(phen)₃]³⁺ (phen = 1,10-phenanthroline).²⁷ It has been found based on the product analysis that there are two pathways for the decay of AcrHR²⁺: one is the C(9)–H bond cleavage (deprotonation) to give AcrR[•] and H⁺, and the other is the C(9)–C bond cleavage to give AcrH⁺ and R[•] as shown in Scheme 1.^{27,42} In the case of $R = \text{H}, \text{Me}, \text{Et}, \text{Ph}$, and CH_2COOEt , the C(9)–H bond is cleaved exclusively to yield only AcrR[•].²⁷ In such a case the decay rate constant of AcrHR²⁺ corresponds to the deprotonation rate constant (k_d). The k_d values thus determined from the decay of AcrHR²⁺ are also listed in Table 1. In contrast, the C(9)–C bond of AcrHR²⁺ is cleaved selectively in the case of $R = \text{Bu}^t$ and CMe_2COOMe when the deprotonation rates were too slow to be determined.^{27,42} In the case of $R = \text{CH}_2\text{Ph}$, $1\text{-CH}_2\text{C}_{10}\text{H}_7$, $\text{CMe}(\text{H})\text{COOEt}$, Pr^i , and CHPh_2 , both the C–H and C–C bonds of AcrHR²⁺ are cleaved to yield two types of products shown in Scheme 1.²⁷ In this case the decay rate constant of AcrHR²⁺ includes the rate constants of two pathways. In the case of $R = \text{CH}_2\text{Ph}$, the deprotonation rate constant (k_d) could be separated from the rate constant of the C–C bond cleavage based on the reaction of AcrHCH₂Ph²⁺ with a base.⁴³ The k_d value of AcrHCH₂Ph²⁺ is also listed in Table 1.

The $\log k_{\text{obs}}$ values of the hydride transfer from AcrHR to a hydride acceptor (A: DDQ or TCNE in eq 4) are plotted against the $\log k_d$ values of the deprotonation of AcrHR²⁺ in Figure 4a, where a reasonably good linear correlation between them is observed except for $R = \text{Ph}$ and CH_2COOEt . Such a linear correlation indicates that the hydride transfer proceeds via

(42) The C(9)–C bond cleavage of AcrHBu^t²⁺ generated by the electrochemical oxidation of AcrHBu^t has also been reported: Anne, A.; Fraoua, S.; Moiroux, J.; Savéant, J.-M. *J. Am. Chem. Soc.* **1996**, *118*, 3938.

(43) The k_d value of AcrHCH₂Ph²⁺ was determined from the k_d value of AcrHMe²⁺ and the ratio of the observed second-order rate constant for the proton transfer from AcrHCH₂Ph²⁺ to 3,5-dichloropyridine to that from AcrHMe²⁺; see ref 27. The k_d values of AcrHR²⁺ in which the C(9)–C bond is cleaved exclusively have not been determined accurately.

(44) The proton transfer cannot precede the initial electron transfer from AcrHR to DDQ, since no deprotonation of AcrHR occurs in the presence of pyridine which is a much stronger base than DDQ.

(45) Fukuzumi, S.; Tokuda, Y. *J. Phys. Chem.* **1992**, *96*, 8409.

(46) Hapiot, P.; Moiroux, J.; Savéant, J.-M. *J. Am. Chem. Soc.* **1990**, *112*, 1337.

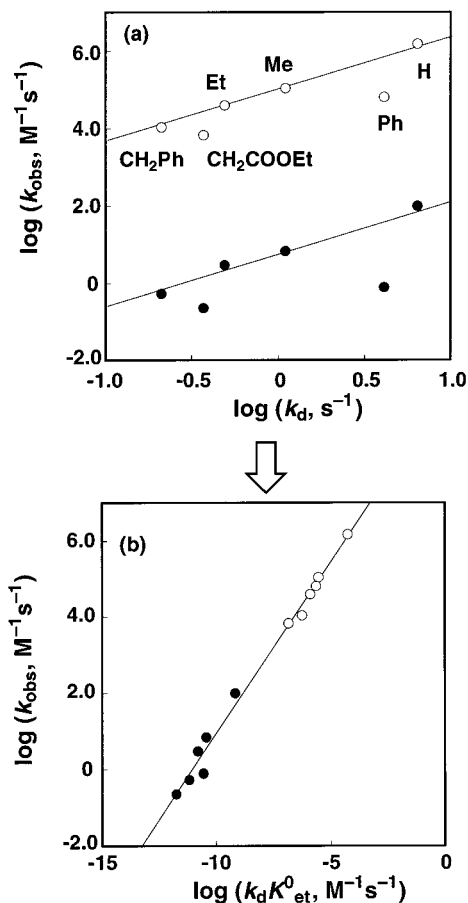
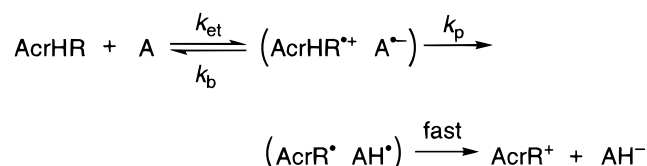


Figure 4. (a) Plots of k_{obs} for the reaction of AcrHR with DDQ (○) and TCNE (●) vs k_d for deprotonation of AcrHR²⁺ in MeCN at 298 K. (b) Plots of k_{obs} for the reaction of AcrHR with DDQ (○) and TCNE (●) vs $k_d K_{\text{et}}^0$.

Scheme 2



electron transfer from AcrHR to A, followed by proton transfer from AcrHR^{•+} to A^{•-} in the radical ion pair and the subsequent electron transfer from AcrR[•] to AH^{•-}, and that the proton-transfer step may be involved as a rate-determining step.⁴⁴ Such a sequential electron–proton–electron transfer leads to the overall hydride transfer to yield AcrR⁺ and AH⁻ (Scheme 2).

Since the one-electron reduction potential of DDQ (E_{red}^0 (vs SCE) = 0.51 V)⁶ or TCNE (E_{red}^0 (vs SCE) = 0.22 V)⁴⁵ is less positive than the one-electron oxidation potential of examined AcrHR (E_{ox}^0 (vs SCE) = 0.81–0.92 V in Table 1),^{6,46} the back electron transfer from A^{•-} to AcrHR^{•+} may be much faster than the proton transfer from AcrHR^{•+} to A^{•-} ($k_b \gg k_p$ in Scheme 1). In such a case, the observed rate constant (k_{obs}) of the overall hydride transfer is given by eq 9, where $K_{\text{et}} = k_{\text{et}}/k_b$, provided that an electron transfer from AcrR[•] to AH^{•-} in the final step in Scheme 1 is much faster than the proton transfer from AcrHR^{•+} to A^{•-}.

$$k_{\text{obs}} = k_p K_{\text{et}} \quad (9)$$

The fast electron transfer from AcrR[•] to AH^{•-} is well supported by the highly negative one-electron oxidation potential of AcrH[•]

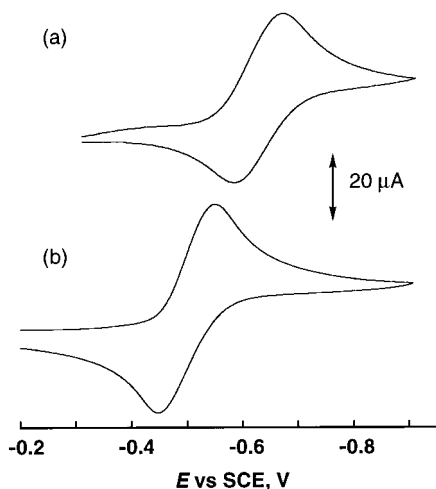


Figure 5. Cyclic voltammograms of (a) AcrPr⁺ClO₄⁻ (1.0 × 10⁻³ M) and (b) AcrCH₂Ph⁺ClO₄⁻ (1.0 × 10⁻³ M) in deaerated MeCN containing TBAP (0.10 M) with a Pt electrode at 298 K; sweep rate 50 mV s⁻¹.

Table 2. One-Electron Reduction Potentials (E^0_{red}) of AcrR⁺ClO₄⁻ Determined by the Cyclic Voltammograms in MeCN at 298 K and the Sweep Rates

AcrR ⁺ , R =	E^0_{red} (vs SCE), V	sweep rate, V s ⁻¹
H	-0.46	15000 ^a
PhCH ₂	-0.50	0.05
Ph	-0.55	0.05
Et	-0.57	1
Bu ^t	-0.59	1
Pr ⁱ	-0.63	0.05

^a Taken from ref 46.

($E^0_{\text{ox}} = -0.46$ V),⁴⁶ which is much more negative than the one-electron reduction potential of A (E^0_{red} (vs SCE) = 0.51 and 0.22 V for DDQ and TCNE, respectively), and these E^0_{red} values are even less positive than the reduction potential of the protonated form of the radical anion (AH[•]).⁴⁷ The E^0_{ox} values of 9-substituted 10-methylacridinyl radicals (AcrR[•]: R = Ph, Et, CH₂Ph, Prⁱ, and Bu^t) are readily determined from the cyclic voltammograms of AcrR⁺, since AcrR[•] is much more stable than AcrH[•] (R = H). The typical cyclic voltammograms are shown in Figure 5 and the E^0_{ox} values of AcrR[•] are listed in Table 2. The E^0_{ox} value of AcrR[•] is more negative than the value of AcrH[•]. Thus, electron transfer from AcrR[•] to AH[•] is highly exergonic irrespective of the type of R (e.g., $\Delta G^0_{\text{et}} < -97$ kJ mol⁻¹ for the AcrCH₂Ph⁺-DDQH[•] system). On the other hand, the proton transfer from AcrH₂²⁺ to DDQ⁻ is known to be endergonic (27 kJ mol⁻¹).⁶ The pK_a value of AcrHBu^t^{•+} may be slightly larger than the pK_a value of AcrH₂²⁺, since the difference in the calculated heat of formation between AcrBu^t[•] and AcrHBu^t^{•+} is slightly (2.3 kJ mol⁻¹) larger than that between AcrH[•] and AcrH₂²⁺.⁴⁸ Thus, the proton transfer from AcrHR²⁺ to A^{•-} should be rate determining as compared to fast electron transfer from AcrR[•] to AH[•] as shown in Scheme 2.

According to eq 9, deviation from linear correlations between log k_{obs} and log k_{d} may be ascribed to the difference in the K_{et} value, since the proton-transfer rate constant (k_{p}) in Scheme 2 may be in parallel with the deprotonation rate constant (k_{d}) in Scheme 1. The equilibrium constant for electron transfer from AcrHR to A (K^0_{et}) to produce free AcrHR²⁺ and A^{•-} can be

(47) Rich, P. R.; Bendall, D. S. *Biochim. Biophys. Acta* **1980**, *592*, 506.

(48) The heats of formation of AcrR[•] and AcrHR²⁺ (R = H and Bu^t) were calculated by the PM3 method.

obtained from the E^0_{ox} value of AcrHR and the E^0_{red} value of A by eq 10. When the difference in the K^0_{et} values for the

$$K^0_{\text{et}} = \exp[-F(E^0_{\text{ox}} - E^0_{\text{red}})/RT] \quad (10)$$

AcrHR-DDQ and AcrHR-TCNE systems is included in the plots between log k_{obs} and log k_{d} , the two separate linear correlations and deviation from the linear lines in Figure 4a are remarkably merged into a single line with a slope of unity as shown in Figure 4b where the log k_{obs} values are plotted against the log $k_{\text{d}}K^0_{\text{et}}$ values.⁴⁹ Thus, it can be concluded that the overall hydride transfer from AcrHR to A proceeds via sequential electron-proton-electron transfer in which the initial electron transfer to produce the radical ion pair is in equilibrium and the proton transfer from AcrHR²⁺ to A^{•-} is the rate-determining step (Scheme 2). The observed primary kinetic isotope effects ($k_{\text{H}}/k_{\text{D}}$) of the overall hydride transfer from AcrH₂ and the 9,9'-dideuterated compound (AcrD₂) to *p*-benzoquinone derivatives (Q)⁵⁰ can be attributed to those of the proton-transfer step from AcrH₂²⁺ and AcrD₂²⁺ to Q^{•-}, since the variation of $k_{\text{H}}/k_{\text{D}}$ with *p*-benzoquinone derivatives has been well correlated with the difference in the pK_a values between AcrH₂²⁺ and QH[•] (ΔpK_{a}) and the maximum value ($k_{\text{H}}/k_{\text{D}} = 10.4$) is obtained at $\Delta pK_{\text{a}} = 0$.⁵⁰

It should be noted that A^{•-} is formed as a final product by the subsequent fast reaction of AH[•] with A (eq 2) and the disproportionation reaction of AH[•] (eq 3) after the overall hydride transfer reaction (eq 1). Such fast reactions following the hydride transfer to produce A^{•-} have precluded the detection of A^{•-} in the course of the hydride-transfer reaction. Conversely the detection of radical ions in hydride-transfer reactions does not necessarily mean the involvement of an electron-transfer step in the hydride-transfer reactions.

CT Complex Formed between AcrHR and *p*-Benzoquinone Derivatives. Although there is an excellent single linear correlation between log k_{obs} and log $k_{\text{d}}K^0_{\text{et}}$, the k_{obs} values, which correspond to the $k_{\text{p}}K_{\text{et}}$ values in eq 9, are 10⁹ times larger than the corresponding $k_{\text{d}}K^0_{\text{et}}$ values (Figure 4). The reason for such a huge difference in the absolute values may be 2-fold. First, the rate constant of proton transfer from AcrHR²⁺ to A^{•-} (k_{p}) may be much larger than the spontaneous deprotonation rate constant of AcrHR²⁺ (k_{d}), since A^{•-} acts as a base. This may be the reason why the proton transfer from AcrHBu^t^{•+} to A^{•-} preceded the cleavage of the C(9)-C bond of AcrHBu^t^{•+} leading to the overall hydride transfer reaction (eq 4). Second, the K_{et} value for the radical ion pair formation in Scheme 2 may also be larger than the K^0_{et} value for formation of free radical ions (AcrHR²⁺ and A^{•-}), since there may be a significant Coulombic interaction between AcrHR²⁺ and A^{•-} in the radical ion pair.⁶

Formation of a radical ion pair is usually preceded by formation of a charge-transfer (CT) complex between an electron donor and acceptor.^{18-22,51} The observation of CT complexes is difficult in fast reactions such as hydride transfer from AcrH₂ to DDQ because of the instability of the CT complex. When

(49) The k_{obs} values are about 10¹⁰ times larger than the corresponding $k_{\text{d}}K^0_{\text{et}}$ values (Figure 4b). Such a large difference may originate from the much larger rate constant of proton transfer from AcrHR²⁺ to a strong base (A^{•-}) than the spontaneous deprotonation rate constant k_{d} , combined with the larger K_{et} value for the radical ion pair formation, in which the large work term is included,⁶ than the K^0_{et} value for the free radical ion formation.

(50) Ishikawa, M.; Fukuzumi, S. *J. Chem. Soc., Faraday Trans.* **1990**, *86*, 3531.

(51) (a) Fukuzumi, S.; Kochi, J. K. *J. Am. Chem. Soc.* **1980**, *102*, 7290. (b) Fukuzumi, S.; Wong, C. L.; Kochi, J. K. *J. Am. Chem. Soc.* **1980**, *102*, 2928. (c) Fukuzumi, S.; Kochi, J. K. *J. Am. Chem. Soc.* **1982**, *104*, 7599.

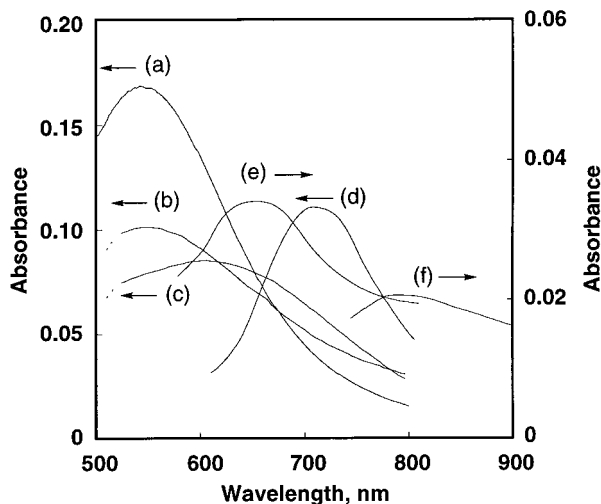


Figure 6. Electronic absorption spectra of CT complexes of (a) AcrH₂ (5.9×10^{-2} M) with chloro-*p*-benzoquinone (6.0×10^{-2} M), (b) AcrHCH₂Ph (1.2×10^{-2} M) with chloro-*p*-benzoquinone (6.0×10^{-2} M), (c) AcrHCH₂Ph (1.2×10^{-2} M) with 2,6-dichloro-*p*-benzoquinone (6.0×10^{-2} M), (d) AcrH₂ (5.9×10^{-2} M) with *p*-chloranil (1.0×10^{-2} M), (e) AcrHBU^t (6.0×10^{-3} M) with *p*-chloranil (1.0×10^{-2} M), and (f) AcrHBU^t (6.0×10^{-3} M) with DDQ (1.0×10^{-2} M) in MeCN at 298 K.

DDQ is replaced by a weaker electron acceptor such as chloro-*p*-benzoquinone, a new broad absorption band, which is characteristic of an intermolecular CT transition, is readily observed upon mixing an MeCN solution of AcrH₂ with that of chloro-*p*-benzoquinone as shown in Figure 6a. When AcrH₂ is replaced by AcrHCH₂Ph, a broad absorption band with the same absorption maximum ($\lambda_{\max} = 540$ nm) is observed (Figure 6b). The λ_{\max} values are shifted to longer wavelengths when chloro-*p*-benzoquinone is replaced by 2,6-dichloro-*p*-benzoquinone and *p*-chloranil which are stronger electron acceptors than chloro-*p*-benzoquinone as shown in Figure 6, lines c and d, respectively. A stopped-flow technique was used for the detection of an unstable CT complex formed between AcrHCH₂Ph and *p*-chloranil (see the Experimental Section). The CT complex is significantly stabilized when AcrHBU^t is employed as an electron donor which has the least reactivity toward hydride acceptors (Table 1). Thus, the CT spectra of AcrHBU^t-*p*-chloranil and AcrHBU^t-DDQ complexes are readily observed as shown in Figure 6, lines e and f, respectively.⁵²

The CT transition energies ($h\nu_{\max}$) observed in Figure 6 are compared with those of other known CT complexes formed between a variety of electron donors and *p*-benzoquinone derivatives^{16,18,53} in Figure 7 where the $h\nu_{\max}$ values are plotted against the difference between the one-electron oxidation potentials of electron donors^{16,54,55} and the one-electron reduction potential of *p*-benzoquinone derivatives,⁶ which is related to

(52) The examined concentration of AcrHBU^t (6.0×10^{-3} M) was smaller than the AcrH₂ concentration (5.9×10^{-2} M) because of the lower solubility of AcrHBU^t, when the CT absorbances of the AcrHBU^t-*p*-chloranil and AcrHBU^t-DDQ complexes in Figure 6, lines e and f, respectively, are smaller than that of the AcrH₂-*p*-chloranil complex (Figure 6d).

(53) (a) Foster, R.; Thomson, T. J. *Trans. Faraday Soc.* **1962**, *58*, 860. (b) Zweig, A.; Lancaster, J. E.; Neglia, M. T.; Jura, W. H. *J. Am. Chem. Soc.* **1964**, *86*, 4130.

(54) Fukuzumi, S.; Hironaka, K.; Nishizawa, N.; Tanaka, T. *Bull. Chem. Soc. Jpn.* **1983**, *56*, 2220.

(55) (a) Mann, C. K.; Barnes, K. K. *Electrochemical Reactions in Nonaqueous Systems*; Marcel Dekker: New York, 1970. (b) Seo, E. T.; Nelson, R. F.; Fritsch, J. M.; Marcoux, L. S.; Leedy, D. W.; Adams, R. N. *J. Am. Chem. Soc.* **1966**, *84*, 3498. (c) Bock, C. R.; Connor, J. A.; Gutierrez, A. R.; Meyer, T. J.; Whitten, D. G.; Sullivan, B. P.; Nagle, J. K. *J. Am. Chem. Soc.* **1979**, *101*, 4815.

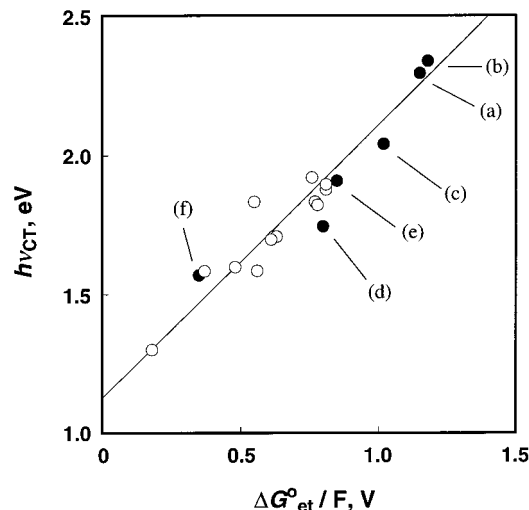
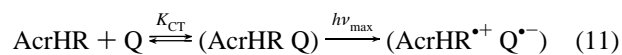


Figure 7. Plot of CT transition energies ($h\nu_{CT}$) of AcrHR-Q complexes (●) and other known CT complexes of Q (○) vs $E_{\text{ox}}^0 - E_{\text{red}}^0$. The $h\nu_{CT}$ and $E_{\text{ox}}^0 - E_{\text{red}}^0$ values are given in the Supporting Information.

the free energy change of electron transfer $\Delta G_{\text{et}}^0/F = E_{\text{ox}}^0 - E_{\text{red}}^0$. The $h\nu_{\max}$ values of the examined AcrHR-*p*-benzoquinone derivative complexes are consistent with those of other known CT complexes in the correlation with $\Delta G_{\text{et}}^0/F$ values (Figure 7). Thus, the observed CT complexes in the course of hydride-transfer reactions from AcrHR to *p*-benzoquinone derivatives (Q) are classified as donor-acceptor complexes of a quite general kind as shown in eq 11.



The formation constant K_{CT} of the CT complex formed between AcrHCH₂Ph and chloro-*p*-benzoquinone (ClQ) in MeCN was determined from an increase in the CT absorbance (A) at λ_{\max} with an increase in the quinone concentration [Q] according to the Benesi-Hildebrand equation (eq 12),⁵⁶ where ϵ is the extinction coefficient. The K_{CT} values were determined at various temperatures. From the plot of $\ln K_{CT}$ vs T^{-1} shown

$$A = \epsilon K_{CT} [\text{AcrHR}] [\text{ClQ}] / (1 + K_{CT} [\text{ClQ}]) \quad (12)$$

in Figure 8 is determined the heat of formation of the CT complex ($\Delta H_{CT} = -29$ kJ mol⁻¹).

Negative Temperature Dependence of the Rates of Hydride Transfer. The decay of the transient CT band observed in the course of the hydride transfer from AcrH₂ to *p*-chloranil in Figure 6d coincides completely with the rise of the absorption band due to the product (see the Supporting Information). However, such a coincidence does not necessarily mean that the CT complex is an intermediate for the hydride transfer reaction as discussed in the Introduction. Whether the observed CT complex is a real intermediate for the hydride transfer reaction or a merely innocent bystander in an otherwise dead-end equilibrium could only be distinguishable by the temperature dependence of the rate if one can observe the negative temperature dependence.

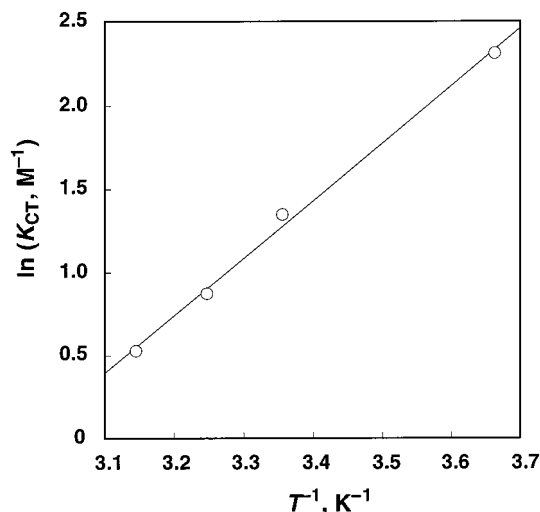
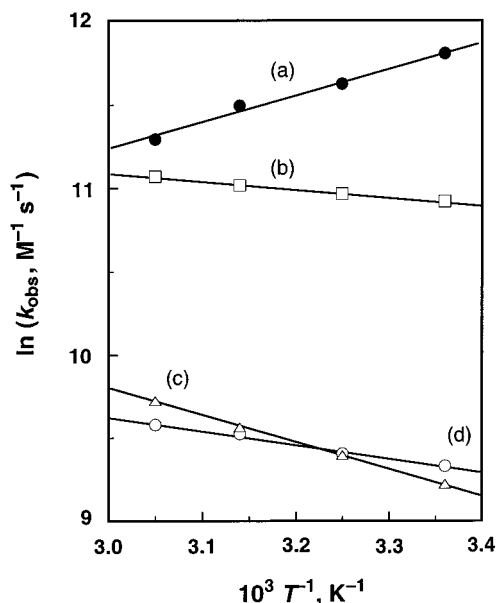
The k_{obs} values for the hydride transfer reaction from AcrHCH₂Ph to DDQ in different solvents were determined at various temperatures and they are listed in Table 3. From the Arrhenius plots shown in Figure 9 are obtained the activation enthalpies ($\Delta H_{\text{obs}}^\ddagger$), and the activation entropies ($\Delta S_{\text{obs}}^\ddagger$) as also

(56) Benesi, H. A.; Hildebrand, J. H. *J. Am. Chem. Soc.* **1949**, *71*, 2703.

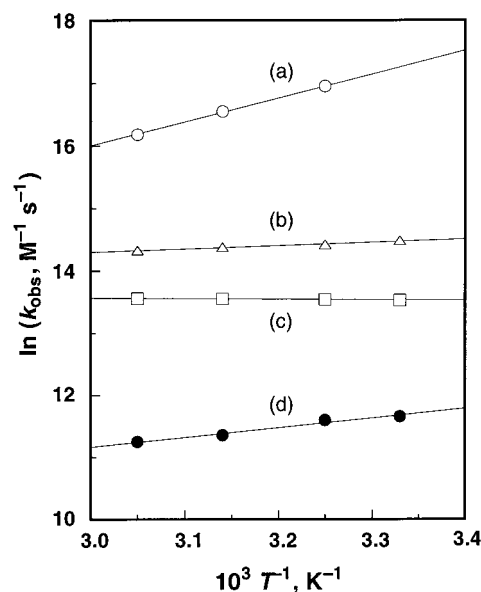
Table 3. Rate Constants of Hydride Transfer Reaction from AcrHCH₂Ph to DDQ in Various Solvents at Different Temperatures, Dielectric Constants, and Activation Parameters

solvent	ϵ	$k_{\text{obs}}, \text{M}^{-1} \text{s}^{-1}$				$\Delta H_{\text{obs}}^{\ddagger}$, kJ mol ⁻¹	$\Delta S_{\text{obs}}^{\ddagger}$, J K ⁻¹ mol ⁻¹
		298 K	308 K	318 K	328 K		
CHCl ₃	4.8	1.3×10^5	1.1×10^5	9.8×10^4	8.0×10^4	-13	-160
CH ₂ ClCH ₂ Cl	10	5.5×10^4	5.8×10^4	6.1×10^4	6.4×10^4	4	-110
PhCN	25	1.0×10^4	1.2×10^4	1.4×10^4	1.7×10^4	13	-89
MeCN	38	1.1×10^4	1.2×10^4	1.4×10^4	1.4×10^4	7	-110

^a The experimental errors are within $\pm 5\%$.

**Figure 8.** Plot of $\ln K_{\text{CT}}$ vs T^{-1} for the temperature dependence of K_{CT} of the CT complex formed between AcrHCH₂Ph and chloro-*p*-benzoquinone in MeCN.**Figure 9.** Arrhenius plots of k_{obs} for the reaction of AcrHCH₂Ph (1.1×10^{-5} M) with DDQ (2.0×10^{-4} M) in (a) CHCl₃, (b) CH₂ClCH₂Cl, (c) PhCN, and (d) MeCN.

listed in Table 3. The k_{obs} value in CHCl₃, which is the least polar solvent among the examined solvents, is the largest. The negative $\Delta H_{\text{obs}}^{\ddagger}$ value (-13 kJ mol⁻¹) is obtained in CHCl₃, and this means *the lower the temperature, the faster the rate of hydride transfer*. The $\Delta H_{\text{obs}}^{\ddagger}$ and $\Delta S_{\text{obs}}^{\ddagger}$ values of other AcrHR derivatives (R = H, Me, and Et) were also determined from the temperature dependence of k_{obs} . The Arrhenius plots are shown in Figure 10, where a negative temperature dependence is clearly observed for the hydride transfer reaction of AcrH₂.

**Figure 10.** Arrhenius plots of k_{obs} for the reaction of AcrHR [R = (a) H, (b) Me, (c) Et, and (d) CH₂Ph; 1.1×10^{-5} M] with DDQ (2.0×10^{-4} M) in CHCl₃.**Table 4.** Rate Constants of Hydride Transfer Reaction from AcrHR to DDQ in CHCl₃ at Different Temperatures and the Activation Parameters

AcrHR, R =	$k_{\text{obs}},^a \text{M}^{-1} \text{s}^{-1}$				$\Delta H_{\text{obs}}^{\ddagger}$, kJ mol ⁻¹	$\Delta S_{\text{obs}}^{\ddagger}$, J K mol ⁻¹
	298 K	308 K	318 K	328 K		
H	<i>b</i>	2.3×10^7	1.6×10^7	1.1×10^7	-32	-170
Me	2.0×10^6	1.8×10^6	1.8×10^6	1.7×10^6	-4	-100
Et	7.5×10^5	7.6×10^5	7.7×10^5	7.8×10^5	1	-95

^a The experimental errors of k_{obs} are within $\pm 5\%$. ^b Too fast to be determined accurately.

The $\Delta H_{\text{obs}}^{\ddagger}$ value of AcrHR increases in the following order: R = H (-32 kJ mol⁻¹) < R = Me (-4 kJ mol⁻¹) < R = Et (1 kJ mol⁻¹), as listed in Table 4.

The observed negative $\Delta H_{\text{obs}}^{\ddagger}$ values, which should be equal to $\Delta H_{\text{CT}} + \Delta H_1^{\ddagger}$ ($k_{\text{obs}} = k_1 K_{\text{CT}}$), could only arise when the CT complex lies along the reaction pathway (vide supra, eq 1). The ΔH_{CT} values for the AcrHR–DDQ complexes may be more negative than the observed ΔH_{CT} value (-29 kJ mol⁻¹) for the AcrH₂ complex with chloro-*p*-benzoquinone, which is a weaker electron acceptor than DDQ. Thus, the heat of formation of the CT complex ($\Delta H_{\text{CT}} < 0$) may be of greater magnitude than the activation enthalpy for the passage of the CT complex to the transition state ($\Delta H_1^{\ddagger} > 0$) in eq 1, i.e., $-\Delta H_{\text{CT}} > \Delta H_1^{\ddagger}$ when the $\Delta H_{\text{obs}}^{\ddagger}$ values ($\Delta H_{\text{obs}}^{\ddagger} = \Delta H_{\text{CT}} + \Delta H_1^{\ddagger}$) become negative. As demonstrated by a single correlation between $\log k_{\text{obs}}$ and $\log(k_{\text{d}} K_{\text{et}}^0)$ in Figure 4b, the ΔH_1^{\ddagger} value for the hydride transfer reaction consists of the sum of the activation enthalpies for electron transfer from AcrHR to DDQ in the CT complex and proton transfer from AcrHR^{•+} to DDQ^{•-} in the radical ion pair in Scheme 2. Thus, the largest negative $\Delta H_{\text{obs}}^{\ddagger}$ value (-32 kJ

mol^{-1}) is obtained for the reaction of AcrH_2 with DDQ when both electron transfer and proton transfer are fastest among examined AcrHR and *p*-benzoquinone derivatives and the ΔH^\ddagger_1 value is therefore minimized. An increase in the $\Delta H^\ddagger_{\text{obs}}$ value of AcrHR in the order $\text{R} = \text{H}$ (-32 kJ mol^{-1}) < $\text{R} = \text{Me}$ (-4 kJ mol^{-1}) < $\text{R} = \text{Et}$ (1 kJ mol^{-1}) in Table 4 can be well accounted for by an increase in the activation enthalpy for the proton-transfer step from $\text{AcrHR}^{*\dagger}$ to DDQ^{*-} , since the deprotonation rate constant of $\text{AcrHR}^{*\dagger}$ decreased in the same order (Table 1). The solvent effects on $\Delta H^\ddagger_{\text{obs}}$ are more complicated than the substituent effects. The more polar the solvent, the more favorable the charge transfer and electron-transfer steps, but the less favorable the proton-transfer step following the electron-transfer step.⁵⁷ These two opposite effects may be optimized in CHCl_3 so as to achieve the smallest ΔH^\ddagger_1 value resulting in the successful observation of the negative $\Delta H^\ddagger_{\text{obs}}$ value in this solvent (Table 2).

Summary and Conclusions

The observed negative temperature dependence of the rate of hydride transfer from AcrH_2 to DDQ gave unequivocal evidence for the role of the observed CT complex as an actual intermediate in the hydride-transfer reaction. The magnitude of the observed rate constant for the reactions of AcrHR with a hydride acceptor (DDQ or TCNE) varies significantly depending on the type of substituent R in AcrHR at the C-9 position and spans a range of 10^7 starting from $\text{R} = \text{H}$ to Bu^t and $\text{CMe}_2\text{-COOMe}$. Such large variation in the rate constant is well

(57) Manring, L. E.; Peters, K. S. *J. Am. Chem. Soc.* **1985**, *107*, 6452.

(58) Theoretical confirmation of the participation of a CT complex as a real intermediate has recently been reported for the Diels–Alder reaction of anthracene with TCNE in which an electron-transfer process following the CT complex formation plays an important role in determining the overall reactivity;^{20c} Wise, K. E.; Wheeler, R. A. *J. Phys. Chem. A* **1999**, *103*, 8279.

correlated with the large variation in the deprotonation rate constant of $\text{AcrHR}^{*\dagger}$ combined with the small variation in the electron-transfer reactivity of AcrHR. On the basis of these results it is concluded that the overall hydride transfer proceeds via a CT complex formed between AcrHR and the hydride acceptor (A), electron transfer from AcrHR to A in the CT complex, proton transfer from $\text{AcrHR}^{*\dagger}$ to A^{*-} , and electron transfer from AcrR^* to AH^* to yield AcrR^+ and AH^- . The overall reactivity is determined by the three consecutive steps, i.e., the CT complex formation, the electron-transfer, and the proton-transfer steps, since the electron transfer in the final step is much faster than the previous proton-transfer step. The initial electron-transfer step in the CT complex may be facilitated by the charge-transfer interaction in the CT complex, since such charge-transfer interaction should result in a decrease in the difference of nuclear configurations before and after the electron-transfer step. Thus, this study has provided the first comprehensive and confirmative understanding of the mechanism of sequential electron–proton–electron transfer via CT complexes.⁵⁸

Acknowledgment. This work was partially supported by a Grant-in-Aid for Scientific Research Priority Area (Nos. 11228205, 11166241, 11136229, and 11555230) from the Ministry of Education, Science, Culture and Sports, Japan.

Supporting Information Available: Decay and the rise of absorbances at 710 and 550 nm due to the AcrH_2 –*p*-chloranil complex and *p*-chloranil radical anion, respectively, in the reaction of AcrH_2 with *p*-chloranil (Figure S1) and a table of $h\nu_{\text{CT}}$ and $E^0_{\text{ox}} - E^0_{\text{red}}$ values plotted in Figure 7 (Table S1) (PDF). This material is available free of charge via the Internet at <http://pubs.acs.org>.

JA9941375